Theory of Two Threshold Fields for Relativistic Runaway Electrons

Pavel Aleynikov*
ITER Organization, Route de Vinon-sur-Verdon, CS 90 046, 13067 St. Paul Lez Durance Cedex, France

Boris N. Breizman†
Institute for Fusion Studies, The University of Texas, Austin, Texas 78712, USA

(Received 28 November 2014; published 14 April 2015)

This Letter presents a rigorous kinetic theory for relativistic runaway electrons in the near critical electric field in tokamaks. The theory provides a distribution function of the runaway electrons, reveals the presence of two different threshold electric fields, and describes a mechanism for hysteresis in the runaway electron avalanche. Two different threshold electric fields characterize a minimal field required for sustainment of the existing runaway population and a higher field required for the avalanche onset. The near-threshold regime for runaway electrons determines the time scale of toroidal current decay during runaway mitigation in tokamaks.

DOI: 10.1103/PhysRevLett.114.155001 PACS numbers: 52.55.Fa, 52.27.Ny

Introduction.—The importance of runaway electron production in plasma was recognized more than a half century ago in a seminal work by Dreicer [1], followed by enlightening subsequent studies by Gurevich [2]. The initial nonrelativistic results [1,2] have been generalized to the relativistic case by Connor and Hastie [3]. Similar to the previous work, Ref. [3] is based entirely on a diffusive (small scattering angle) approximation for Coulomb collisions. The missing large-angle (knockon) collisions are known to be weak compared to the small-angle collisions, but they can cause an avalanche-type growth of the runaway population, as pointed out in Ref. [4] and substantiated in Refs. [5,6]. In the absence of an external magnetic field, the electric field can accelerate runaway electrons until they reach the pair-production energy range, but in magnetically confined plasmas the runaway energies are limited, rather, by synchrotron losses that accompany pitch-angle scattering. The significance of this mechanism was first shown in Ref. [7] and then emphasized in Refs. [8,9].

The compelling need to mitigate runaway electrons or to control their behavior in ITER calls for additional attention to the abovementioned aspects of the runaway problem: relativistic energies of the runaways, avalanche mechanism of the runaway production, and the combined effect of pitch-angle scattering and synchrotron losses on the runaway distribution function (this effect was omitted in Ref. [6]). It is especially important to have an accurate theory for the near-threshold regime that represents long-term behavior of the runaways and is critical for the mitigation process. Even a very strong initial inductive electric field is reasonably expected to drop down to the threshold-level values with the growth of the runaway population. The key questions in that regard are: what is the threshold electric field and what is the growth rate of the avalanche when the electric field exceeds the threshold? The threshold electric field must at least overcome the collisional friction for ultrarelativistic electrons, which means that this field cannot be less than

$$E_c = \frac{e^3 n_e \Lambda}{4\pi\varepsilon_0^2 m_0 c^2}. \tag{1}$$

This expression is commonly referred to as the critical field for runaway avalanche, but there are strong experimental indications [10,11] that it actually underestimates the avalanche threshold considerably, and prior theoretical work [7] partly attributes the difference to synchrotron losses. However, the simple dynamical model used in Ref. [7] to explain the role of synchrotron losses is too crude for quantitative predictions. To enable such predictions, we now present a systematic kinetic treatment of the problem, which not only refines the findings of Ref. [7] but also provides an accurate description of the runaway distribution function, reveals a mechanism for the hysteresis in the evolution of runaways, and explains the effect of runaways on the current decay process.

Kinetic model.—The rates of the small-angle and large-angle (avalanche-producing) collisions of runaway electrons differ by the large Coulomb logarithm Λ. Because of this difference, the avalanche time scale is relatively slow compared to the small-angle collisional processes, especially at the later stage of runaway formation or during the runaway current mitigation. This separation of time scales suggests a two-step approach to the problems of runaway production and mitigation in the near-threshold regimes. We first ignore the large-angle collisions and study the behavior of preexisting runaways. We then use the distribution function of the accumulated runaways to predict their production and loss. To sidestep the discussion of secondary geometric factors, we consider the runaways in a uniform fully ionized plasma with a uniform magnetic field

B and constant electric field E along the magnetic field lines. The distribution function F satisfies the relativistic Fokker-Planck equation

$$\frac{\partial F}{\partial s}+\frac{\partial}{\partial p}\left[E\cos\theta-1-\frac{1}{p^2}-\frac{p\sqrt{1+p^2}}{\bar{\tau}_{\rm rad}}\sin^2\theta\right]F = \frac{1}{\sin\theta}\frac{\partial}{\partial\theta}\sin\theta\left[E\frac{\sin\theta}{p}F+\frac{(Z+1)}{2}\frac{\sqrt{p^2+1}}{p^3}\frac{\partial F}{\partial\theta}+\frac{1}{\bar{\tau}_{\rm rad}}\frac{\cos\theta\sin\theta}{\sqrt{1+p^2}}F\right], \quad (2)$$

where p is the particle momentum (normalized to mc), θ is the pitch angle, s is the time variable (normalized to $\tau\equiv 4\pi\varepsilon_0^2 m_0^2 c^3/e^4 n_e\Lambda$), E is the electric field (normalized to $m_0 c/e\tau\equiv E_c$), and $\bar{\tau}_{\rm rad}\equiv\tau_{\rm rad}/\tau=(6\pi\varepsilon_0 m_0^3 c^3/e^4B^2)(1/\tau)$ is the normalized time of synchrotron losses. The normalization of the distribution function is given by $\int F dp\sin\theta d\theta=1$. In fully ionized plasmas, Z is the ion charge, whereas in cold postdisruption plasmas with impurities, Z should be adjusted to capture the effects of the fast electron scattering on impurity ions and atomic nuclei. Also, the expression for τ needs to be generalized to take into account collisions with the bound electrons. These generalizations have been discussed in Refs. [12,13].

We note that E is an order of unity quantity and τ is much less than $\tau_{\rm rad}$ for the tokamak parameters we are most interested in. This allows us to drop the last term on the right-hand side of Eq. (2). We next make a conjecture (which is internally consistent for the solution we construct, as can be checked directly afterwards) that the time scale for pitch-angle equilibration is much shorter than the momentum evolution time scale in the near-threshold case, since the momentum convection terms in Eq. (2) (acceleration by the electric field and collisional and radiative drag) are nearly balanced for the electrons of interest when E is close to the avalanche onset threshold denoted below as E_a. The angular distribution of the existing runaways can therefore be found from the condition that pitch-angle scattering balances the pitch-angle shrinking caused by the electric field; i.e., the lowest order version of Eq. (2) is

$$\frac{E}{p}F+\frac{(Z+1)}{2}\frac{\sqrt{p^2+1}}{p^3}\frac{1}{\sin\theta}\frac{\partial F}{\partial\theta}=0, \quad (3)$$

which specifies the angular part of the distribution function, so that

$$F=G(s;p)\frac{A}{2\sinh A}\exp\left[A\cos\theta\right], \quad (4)$$

with

$$A(p)\equiv\frac{2E}{(Z+1)}\frac{p^2}{\sqrt{p^2+1}}, \quad (5)$$

where $A/2\sinh A$ is the normalization factor for the pitch-angle distribution and the function $G(s;p)$ still needs to be determined from Eq. (2). In order to find this function, we integrate Eq. (2) over all pitch angles, which eliminates the lowest order terms and gives a one-dimensional kinetic equation for $G(s;p)$:

$$\frac{\partial G}{\partial s}+\frac{\partial}{\partial p}U(p)G=0, \quad (6)$$

where

$$U(p)\equiv-\left[\frac{1}{A(p)}-\frac{1}{\tanh\left[A(p)\right]}\right]E-1-\frac{1}{p^2}+\frac{Z+1}{E\bar{\tau}_{\rm rad}}\frac{p^2+1}{p}\left[\frac{1}{A(p)}-\frac{1}{\tanh\left[A(p)\right]}\right]. \quad (7)$$

Equation (6) is a continuity equation in the momentum space with a "flow velocity" defined by Eq. (7) and shown in Fig. 1 for three different values of the electric field. This velocity is negative for all momenta if the electric field is lower than a certain threshold value $E_0(Z;\bar{\tau}_{\rm rad})$ (dotted curve in Fig. 1). In other words, any initially created population of fast electrons will slow down and join the bulk if $E<E_0$. In contrast, a higher field ($E>E_0$) creates a finite interval of positive flow velocities (under the solid curve in Fig. 1), which enables sustainment of fast electron population in the plasma. In what follows, E_0 is referred to as the sustainment threshold. For $E>E_0$, the flow velocity vanishes at two equilibrium points ($p_{\rm min}$ and $p_{\rm max}$), of which the higher momentum point is stable and the lower momentum is unstable. More specifically, the electrons slow down and join the bulk if their momenta are less than $p_{\rm min}$, whereas the electrons with larger initial momenta ($p>p_{\rm min}$) move towards $p_{\rm max}$ and accumulate there, so that the entire population of fast electrons eventually concentrates near $p_{\rm max}$. In particular, the electrons with initial momenta higher than $p_{\rm max}$, if any, decelerate towards $p_{\rm max}$. It is essential that this process is faster than the rate of large-angle collisions, which simplifies calculation of the avalanche growth rate significantly.

The function $U(p)$ dictates the applicability condition for the separation of time scales between the pitch-angle equilibration and the momentum evolution. The low value

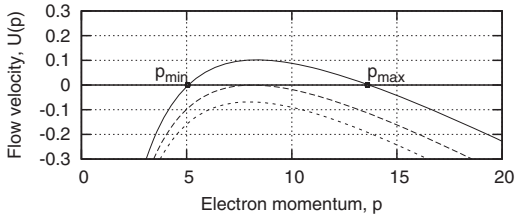

FIG. 1. The flow velocity $U(p)$ defined by Eq. (7) for $Z=5$ and $\bar{\tau}_{\rm rad}=70$. The values of the electric field E are 1.8 for the solid curve, 1.7 for the dashed curve, and 1.65 for the dotted curve.

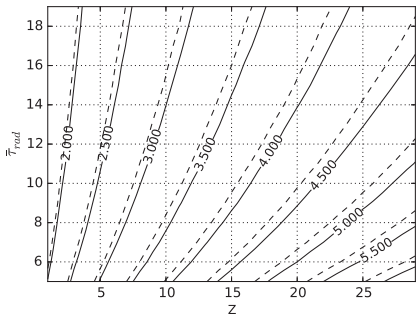

FIG. 2. The contours of the sustainment field E_0 (solid curves) and the avalanche onset field E_a (dashed curves).

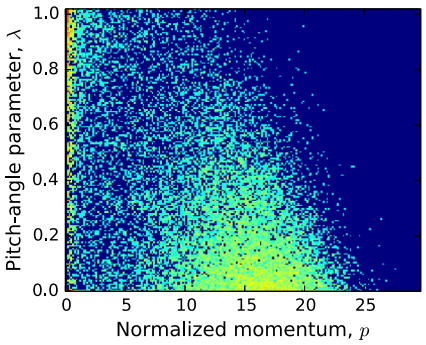

FIG. 3 (color online). Snapshot of the runaway electron distribution in momentum and pitch angle during the decay process. The pitch-angle parameter is $\lambda \equiv \sin^2\theta$.

of $U(p)$ ($U \ll p$) at $p_{\min} < p < p_{\max}$ ensures that the momentum evolution is slower than the pitch-angle equilibration. This is not the case for $p \gg p_{\max}$ and $p \ll p_{\min}$, where Eq. (6) becomes inaccurate. However, such electrons will quickly decelerate toward the region of validity of the presented solution (if $p \gg p_{\max}$) or merge the bulk plasma (if $p \ll p_{\min}$), which enables the prediction of the sustained distribution function.

Note that the stable point $p_{\max}$ would not exist in the absence of synchrotron losses, because the stopping power for ultrarelativistic electrons is nearly constant (we neglect a weak logarithmic rise of the collisional stopping power at high energies). The electrons would then accelerate constantly in a supercritical electric field. Synchrotron losses introduce a momentum-dependent stopping force, which precludes unlimited acceleration of the electrons and thereby sets an upper limit on runaway energies. The sustainment threshold E_0 should not be confused with the critical electric field E_c determined solely by the collisional friction.

The equilibrium points ($p_{\min}$ and $p_{\max}$) merge when the electric field equals E_0 (the flow velocity function for this case is shown by the dashed curve in Fig. 1). This condition serves as a formal definition of E_0. Figure 2 presents the resulting contour plots for E_0 on the $(Z;\bar{\tau}_{\rm rad})$ plane (solid contours). There is also a convenient analytic fit for E_0,

$$E_0 \approx 1 + \frac{\frac{(Z+1)}{\sqrt{\bar{\tau}_{\rm rad}}}}{\sqrt[6]{\frac{1}{8} + \frac{(Z+1)^2}{\bar{\tau}_{\rm rad}}}}, \tag{8}$$

that has better than 5% accuracy for $1 < Z < 30$ and $\bar{\tau}_{\rm rad} > 5$.

Equation (6) predicts significant peaking of the distribution function near the phase-space attractor at $p_{\max}$ for the electric fields greater than E_0 but still in the E_0 range. This peaking is also observed in a Monte Carlo solution of Eq. (2) presented in Ref. [12]. A snapshot of the numerically calculated distribution function in the process of contraction is shown in Fig. 3. The difference between the commonly assumed monotonic distribution of runaways, obtained in Ref. [6], and the peaked distribution should apparently change the avalanche growth, the likelihood of wave excitation by the runaway beam, and the runaway mitigation assessments.

Avalanche growth rate and the hysteresis effect.—The kinetic model described above allows straightforward calculation of the avalanche growth rate. Taking into account the relatively fast electron flow to $p = p_{\max}$, we assume that the relativistic factor for all primary electrons is $\gamma_0 = \sqrt{p_{\max}^2 + 1}$. Let γ be the relativistic factor of an electron after collision of the primary electron with an immobile bulk plasma electron. The differential cross section for their collision is [14]

$$\frac{d\sigma}{d\gamma} = \frac{2\pi r_e^2}{\gamma_0^2 - 1}\left[\gamma_0^2\left(\frac{1}{\gamma - 1}\right)^2 + \gamma_0^2\left(\frac{1}{\gamma_0 - \gamma}\right)^2 + 1 - \frac{2\gamma_0 - 1}{\gamma_0 - 1}\left(\frac{1}{\gamma - 1} + \frac{1}{\gamma_0 - \gamma}\right)\right], \tag{9}$$

where r_e is the classical electron radius.

Recalling the structure of the velocity flow (7), we conclude that the after-collision energies of both electrons need to be greater than $\gamma_{\min} \equiv \sqrt{p_{\min}^2 + 1}$ to produce the avalanche. This ensures that both electrons will flow to the stable point γ_0 after the collision. The energy conservation law limits the values of γ for such collisions to $\gamma_{\min} < \gamma < \gamma_0 + 1 - \gamma_{\min}$. The total cross section for such events is then $\sigma = \int_{\gamma_{\min}}^{\gamma_0 + 1 - \gamma_{\min}} (d\sigma/d\gamma) d\gamma$, and the resulting growth rate of the avalanche is

$$\Gamma \equiv \frac{1}{n_{re}}\frac{\partial n_{re}}{\partial s} = \frac{n_e \sigma c \tau}{2}\frac{\sqrt{\gamma_0^2 - 1}}{\gamma_0}, \tag{10}$$

or, equivalently,

$$\Gamma = \frac{1}{4\Lambda\gamma_0\sqrt{\gamma_0^2 - 1}}\left[-\frac{2\gamma_0 - 1}{\gamma_0 - 1}2\ln\left(1 + \frac{\gamma_0 + 1 - 2\gamma_{\min}}{\gamma_{\min} - 1}\right) + (\gamma_0 + 1 - 2\gamma_{\min})\left(1 + \frac{2\gamma_0^2}{(\gamma_{\min} - 1)(\gamma_0 - \gamma_{\min})}\right)\right]. \tag{11}$$

The factor $1/2$ in Eq. (10) accounts for the fact that each collision involves two electrons, but only one of them can be a new member of the runaway population. As seen from Eq. (11), $\gamma_{\min}$ has to be less than $(\gamma_0+1)/2$ to develop an avalanche, so that the avalanche threshold is determined by the condition $\gamma_0+1-2\gamma_{\min}=0$. The corresponding threshold value E_a of the inductive electric field is greater than E_0 (as indicated by dashed contours in Fig. 2).

If the electric field is lower than E_a, then the growth rate Γ is negative. The large-angle collisions work against the avalanche in this case, because the final energies of the colliding electrons can be less than $\gamma_{\min}$, which forces these electrons to move away from the γ_0 attractor into the bulk. However, the resulting decay of the fast electron population is relatively slow (because of the large Coulomb logarithm). As a result, the finite interval between E_0 and E_a enables long sustainment of the fast electrons without their exponential multiplication. This regime differs significantly from the predictions of the previous avalanche theory [6]. Another important difference is that, for the fields greater than E_0, the rate of runaways production is lower than the one predicted in Ref. [6]. The reason for both differences is a simplified description of the secondary electron source in Ref. [6], which assumes extremely high energies of the primary electrons. The same simplified source was also used in Ref. [9]. This simplification breaks down in the near-threshold regime, where finite energy of the primary electrons needs to be accounted for.

Note that rare large-angle collisions of the attractor runaways with bulk plasma electrons do naturally create an accompanying population of lower energy electrons (with $p<p_{\min}$). This effect was discussed in Refs. [15,16] as a candidate for electrical breakdown in atmosphere. The lower energy electrons are apparent in tokamak experiments, but their effect on the attractor particles should be relatively small due to the large Coulomb logarithm. We therefore omit the discussion of the lower energy electrons in this Letter.

The difference between E_0 and E_a creates a hysteresis in the runaway behavior. If the electric field grows starting from $E<E_0$, there will be no runaways at $E=E_0$, because the avalanche does not start until the field reaches E_a. On the other hand, when the field decreases from $E>E_a$ and there is already a population of the runaways, the avalanche stops at $E=E_a$, but the existing runaways can last as long as the field remains greater than E_0.

Figure 4 presents the avalanche growth rate as a function of the electric field for $Z=5$ and $\bar{\tau}_{\rm rad}=70$. The solid line is the growth rate determined by Eq. (11), and the dashed line represents Eq. (18) from Ref. [6]. We observe that the two results agree when the electric field is several times greater than the critical filed E_c. This is consistent with the fact that the approximate source used in Ref. [6] is sufficiently accurate at high electric fields when the value of γ_0 is very large and the role of synchrotron radiation becomes negligible near the unstable point $p_{\min}$. However,

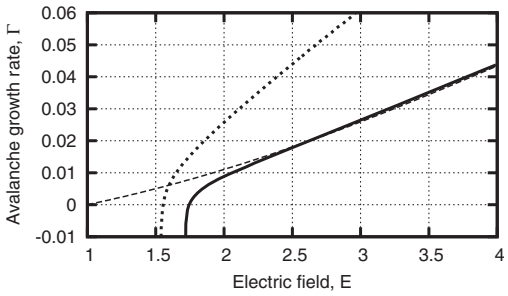

FIG. 4. Avalanche growth rate predicted by Eq. (11) (solid curve) in comparison with Eq. (18) from Ref. [6] (dashed curve) and the growth rate inferred from the dynamical model of Ref. [7] (dotted curve).

at lower electric fields, Eq. (18) from Ref. [6] overestimates the growth rate significantly, and it does not describe the decay of the runaway population, resulting from large-angle scattering at $E_0<E<E_a$.

Note that the approximations used to solve Eq. (2) in the near-threshold regime apparently breaks down at large electric fields, but the avalanche growth rate there is insensitive to the near-threshold subtleties, which explains why Fig. 4 shows close agreement between our calculations and prior results at large fields. To be perfectly accurate, the intermediate range in Fig. 4 should be understood as a sensible interpolation.

It is instructive to compare our kinetic results with the predictions of a truncated dynamical model proposed in Ref. [7]. This model suggests a set of two coupled ordinary differential equations for the average relativistic factor and the pitch-angle parameter. It involves a simplifying conjecture that one can capture interesting qualitative trends by first neglecting all higher moments of the runaway distribution function. Although the dynamical model of Ref. [7] exhibits formation of the phase-space attractor and captures the global pattern of the electron flow in phase space, the value of the threshold electric field obtained from this model is not quite accurate, due to the arbitrariness of the truncation procedure. We also find that the dynamical model (if used for the avalanche growth rate calculation) would give an overestimated value, as shown in Fig. 4. Our kinetic approach is free from these weaknesses.

Current decay.—The runaway avalanche threshold is of primary importance with regard to mitigation of the runaways. The mitigation process involves dissipation of the stored magnetic energy, and the time scale of this process is typically much longer than the characteristic growth time of the runaway avalanche. This separation of time scales means that the inductive electric field must be close to the threshold value E_0 at every flux surface where runaways are present [17]. In a simplified cylindrical geometry, this condition (together with Maxwell equations) immediately gives the time derivative of the *total* current density on every runaway-occupied surface:

$$\frac{\partial j}{\partial t} = \frac{1}{\mu_0}\frac{1}{r}\frac{\partial}{\partial r} r \frac{\partial E_0}{\partial r}, \quad (12)$$

where we now use SI units for all quantities including E_0. We herein ignore the difference between E_0 and E_a, because it is relatively small compared to E_0, as seen in Fig. 2. On every other (runaway-free) flux surface, the electric field must be lower than E_0 and governed by the bulk plasma conductivity σ. Equation (12) can then be generalized to

$$\frac{\partial j}{\partial t} = \frac{1}{\mu_0}\frac{1}{r}\frac{\partial}{\partial r} r \frac{\partial}{\partial r}\left[E_0 + \left(\frac{j}{\sigma} - E_0\right) H\left(E_0 - \frac{j}{\sigma}\right)\right], \quad (13)$$

where H is the Heaviside step function. We observe that the threshold field E_0 sets an upper limit for the rate of magnetic energy dissipation and thereby determines the shortest possible time for the total current decay. A rough estimate of this time is

$$\tau_{\min} \sim \frac{\mu_0 I}{E_0}. \quad (14)$$

We also note that this estimate is insensitive to the energy spectrum of runaway electrons and that the decay should be linear in time [as seen from Eq. (12)] if the runaways occupy most of the plasma cross section and the threshold field does not evolve significantly during the decay process. The expected decay rate and linear time dependence appears to be consistent with what is usually seen in the mitigation experiments [18] if one allows for additional (vessel) inductance that extends the decay time.

Summary.—The presented rigorous theory demonstrates that the electric field for runaway avalanche onset is higher and the avalanche growth rate is lower than previous predictions. The new theory predicts peaking of the runaway distribution function at the phase-space attractor and the existence of two different threshold fields that produce a hysteresis in the runaway evolution. These findings open a possibility for improved interpretation of the corresponding experiments, including interpretation of the x-ray and synchrotron emission measurements. The existence of threshold electric fields for sustainment and growth of the runaway population explains the time evolution of the *total* toroidal current in the runaway mitigation experiments.

This work was supported by the Principality of Monaco/ITER Postdoctoral Fellowship, by ITER under Contract No. ITER-CT-12-4300000273, and by the U.S. Department of Energy Contract No. DEFG02-04ER54742. The views and opinions expressed herein do not necessarily reflect those of the ITER Organization.

*pavel.aleynikov@iter.org
†breizman@mail.utexas.edu

[1] H. Dreicer, Phys. Rev. **115**, 238 (1959); **117**, 329 (1960).
[2] A. V. Gurevich, J. Exp. Theor. Phys. **39**, 1296 (1960).
[3] J. W. Connor and R. J. Hastie, Nucl. Fusion **15**, 415 (1975).
[4] Yu. A. Sokolov, JETP Lett. **29**, 218 (1979).
[5] R. Jayakumar, H. H. Fleischmann, and S. Zweben, Phys. Lett. A **172**, 447 (1993).
[6] M. N. Rosenbluth and S. V. Putvinski, Nucl. Fusion **37**, 1355 (1997).
[7] J. R. Martin-Solis, J. D. Alvarez, R. Sánchez, and B. Esposito, Phys. Plasmas **5**, 2370 (1998).
[8] F. Andersson, P. Helander, and L-G. Eriksson, Phys. Plasmas **8**, 5221 (2001).
[9] A. Stahl, E. Hirvijoki, J. Decker, O. Embreus, and T. Fülöp, Phys. Rev. Lett. **114**, 115002 (2015).
[10] J. R. Martin-Solis, R. Sanchez, and B. Esposito, Phys. Rev. Lett. **105**, 185002 (2010).
[11] R. S. Granetz, B. Esposito, J. H. Kim, R. Koslowski, M. Lehnen, J. R. Martin-Solis, C. Paz-Soldan, T. Rhee, J. C. Wesley, and L. Zeng, Phys. Plasmas **21**, 072506 (2014).
[12] P. Aleynikov, K. Aleynikova, B. Breizman, G. Huijsmans, S. Konovalov, S. Putvinski, and V. Zhogolev, in *Proceedings of the 25th IAEA Fusion Energy Conference, St. Petersburg, Russian Federation, 2014*, pp. TH/P3–38.
[13] V. E. Zhogolev and S. V. Konovalov, VANT series Nuclear Fusion **37**, 71 (2014) [Phys. At. Nucl. (to be published)].
[14] C. Møller, Ann. Phys. (Berlin), **406**, 531 (1932).
[15] A. V. Gurevich, G. M. Milikh, and R. Roussel-Dupre, Phys. Lett. A, **165**, 463 (1992).
[16] J. R. Dwyer and L. P. Babich, J. Geophys. Res. **116**, A09301 (2011).
[17] B. N. Breizman, Nucl. Fusion **54**, 072002 (2014).
[18] E. Hollmann *et al.*, Nucl. Fusion **53**, 083004 (2013).